Nuclear Instruments and Methods in Physics Research A 834 (2016) 132–142

Contents lists available at ScienceDirect

Nuclear Instruments and Methods in Physics Research A

journal homepage: www.elsevier.com/locate/nima

HORACE: Software for the analysis of data from single crystal spectroscopy experiments at time-of-flight neutron instruments

R.A. Ewings [a], A. Buts [a], M.D. Le [a], J. van Duijn [b], I. Bustinduy [c], T.G. Perring [a,d,*]

[a] ISIS Facility, STFC Rutherford Appleton Laboratory, Harwell Campus, Didcot OX11 0QX, UK
[b] Departamento de Mecánica, Universidad de Córdoba, 14071 Córdoba, Spain
[c] ESS Bilbao, Poligono Ugaldeguren III, Pol. A, 7B - 48170 Zamudio, Bizkaia – País Vasco, Spain
[d] London Centre for Nanotechnology and Department of Physics and Astronomy, University College London, Gower Street, London WC1E 6BT, UK

ARTICLE INFO

Article history:
Received 20 April 2016
Received in revised form
8 July 2016
Accepted 16 July 2016
Available online 19 July 2016

Keywords:
Time-of-flight
Neutron spectroscopy
Multidimensional visualization

ABSTRACT

The HORACE suite of programs has been developed to work with large multiple-measurement data sets collected from time-of-flight neutron spectrometers equipped with arrays of position-sensitive detectors. The software allows exploratory studies of the four dimensions of reciprocal space and excitation energy to be undertaken, enabling multi-dimensional subsets to be visualized, algebraically manipulated, and models for the scattering to simulated or fitted to the data. The software is designed to be an extensible framework, thus allowing user-customized operations to be performed on the data. Examples of the use of its features are given for measurements exploring the spin waves of the simple antiferromagnet $RbMnF_3$ and ferromagnetic iron, and the phonons in URu_2Si_2.

1. Introduction

Neutron spectrometers at central facilities around the world are routinely used to measure the wave-vector, $\mathbf{Q}$, and energy, $\hbar\omega$, dependency of the spectrum of lattice dynamics and magnetic excitations, $S(\mathbf{Q}, \omega)$. These data can provide detailed information about the strength, range and symmetry of the interatomic and magnetic interactions, and consequently are highly sensitive tests of theoretical models. The triple-axis spectrometer (TAS) at research reactors has traditionally been the instrument of choice because of its controllability and flexibility [1], whereby the $S(\mathbf{Q}, \omega)$-dependency is explored point-by-point. Over the past 15–20 years time-of-flight spectrometers with position-sensitive detectors (PSDs) have established themselves as extraordinarily effective instruments for measuring excitations in single crystals where the interactions are strong in one or two dimensions, for example in the cuprate and iron-based superconductors, and in quasi one- and two-dimensional model magnetic systems. [2–21]. However, until recently there have been relatively fewer measurements in systems where there are significant interactions in all three spatial dimensions. By combining many separate runs, each with a different crystal orientation, into a single data set, complete measurements of the four-dimensional scattering function $S(\mathbf{Q}, \omega)$ can be made. This has become possible through the combination of the latest instruments with large solid angle position sensitive detector arrays [22–27] and, crucially, optimized software to visualize and manipulate the massive data sets that are created.

Here the software application HORACE is described, which is in routine use, at several neutron facilities, by their users for the visualization and analysis of such data sets. This paper describes the background to the experimental method, and the principles of HORACE are outlined. The features of the software are described in detail, together with a summary of how it is practically used, with examples that illustrate its operation and features. Details of computer hardware requirements, and software download and installation are also summarized.

2. Theory

Fig. 1 shows a schematic diagram of the MERLIN spectrometer [23] at the ISIS spallation neutron source at the STFC Rutherford Appleton laboratory in the UK, an example of the latest generation of direct geometry spectrometers. In this example, a pulse of protons hits the spallation target every 20 ms to produce a pulse of neutrons. These are rapidly slowed down in a moderator to produce a pulse of neutrons with characteristic width measured in microseconds, but with a spread of useable energies in the instrument of ~10 meV to ~ 3 eV. A monochromatic pulse of neutrons with the desired energy E_i is selected by correctly choosing

* Corresponding author at: ISIS Facility, STFC Rutherford Appleton Laboratory, Harwell Campus, Didcot OX11 0QX, UK.
E-mail address: toby.perring@stfc.ac.uk (T.G. Perring).

http://dx.doi.org/10.1016/j.nima.2016.07.036
0168-9002/

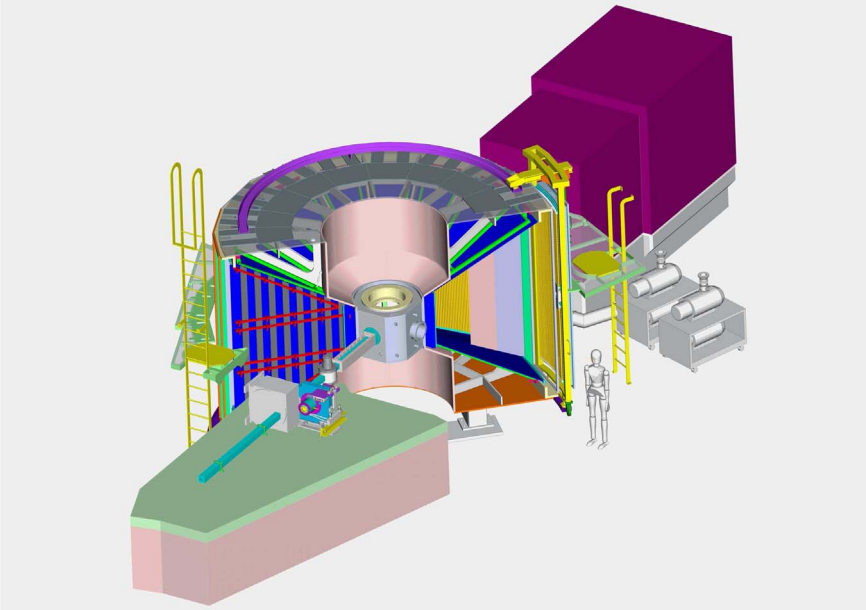

Fig. 1. Schematic of the MERLIN chopper spectrometer, at the ISIS spallation neutron source. A white beam of neutrons from the source moderator is incident from the bottom left in this schematic. The principles of operation are described in the text. Such instruments are ideally suited for the technique of combining multiple datasets, with their high flux and large solid angle detector coverage enabling rapid surveys of the 4D scattering function $S(\mathbf{Q}, \omega)$ to be undertaken.

the phase of a rotating collimator (Fermi chopper), or system of disk choppers, just before the sample. The sample scatters neutrons, and on MERLIN these are collected by a three steradian position sensitive detector array. The time of arrival with respect to the proton pulse of each scattered neutron is recorded together with its location on the detector array. Because the moderator-to-sample distance x_1 is known, as is the sample-to-detector distance x_2 for each detector element, the magnitude of the scattered wave vector for each recorded neutron is determined by the time-of-arrival at the detector, t_{det}:

$$k_f = \frac{m_{\mathrm{N}}}{\hbar}\left(\frac{x_2}{(t_{\mathrm{det}} - t_{\mathrm{samp}})}\right) \tag{1}$$

where $t_{\mathrm{samp}} = (m_{\mathrm{N}}/\hbar)\cdot(x_1/k_i)$ is the time the monochromatic pulse hits the sample, k_i is the magnitude of the incident wave vector given by $E_i = \hbar^2 k_i^2/2m_{\mathrm{N}}$, and m_{N} is the mass of the neutron. The momentum and energy transferred to the sample are then computed [28] as

$$\begin{aligned}\mathbf{Q} &= \mathbf{k}_i - \mathbf{k}_f \\ \hbar\omega &= \frac{\hbar^2}{2m_{\mathrm{N}}}(k_i^2 - k_f^2)\end{aligned} \tag{2}$$

For a chosen k_i and sample orientation, there are three independent degrees of freedom, corresponding to the spherical polar angles θ and ϕ that define the direction of $\mathbf{k}_f$, and the time-of-arrival t_{det} which in turn has a one-to-one correspondence with energy transfer, $\hbar\omega$, or equivalently with $k_f \equiv |\mathbf{k}_f|$. In consequence, the momentum and frequency dependent scattering function $S(\mathbf{Q}, \omega)$ is measured on a 3D manifold in the four dimensions of $\mathbf{Q}$ and ω, with the volume defined by the ranges of θ and ϕ set by the size of the detector array, and $-\infty \le \hbar\omega \le E_i$. Equivalently, in any particular choice of coordinate frame for $\mathbf{Q}$, then of the four coordinates $\{Q_\alpha\} \equiv (\mathbf{Q}, \omega)$ with $Q_\alpha = Q_\alpha(\theta, \phi, t_{\mathrm{det}})$, $\alpha = 1-4$, only three components are independent, with the fourth an implicit function of the other three. We note that a similar line of reasoning can be used for indirect geometry spectrometers, for which the final energy E_f is fixed and the time-of-flight is used to determine k_i.

The physically relevant coordinate frames in which to express the components of $\mathbf{Q}$ are ones that are fixed with respect to the crystal lattice. For example, one may choose the components along the reciprocal lattice vectors $\boldsymbol{a}^*$, $\boldsymbol{b}^*$ and $\boldsymbol{c}^*$. A good choice of coordinate frame and of which component of $\{Q_\alpha\}$ is the implicit coordinate will depend on the material being studied. For example, in some magnetic materials such as the parent high temperature superconductor compound La_2CuO_4 [29], the magnetic ions are arranged in layers, with the magnetic exchange parameters between the layers orders of magnitude weaker than those within the layers. In this case, the best choice of coordinate frame is one with components Q_1 and Q_2 within the layers and Q_3 perpendicular to the layers. Because the interactions between the layers are negligible, $S(\mathbf{Q}, \omega)$ has a simple dependence on Q_3, mainly due to the form factor. In this instance, Q_3 is taken to be the implicit variable, and the intensity as a function of (Q_1, Q_2, ω) gives the relevant information of $S(\mathbf{Q}, \omega)$. Typical plots of $S(\mathbf{Q}, \omega)$ at a constant energy are thus projected along the physically uninteresting Q_3-axis. In quasi-1D magnets, where the interactions are strong only along one direction – label it Q_1 for definiteness – then Q_3 can be ignored as the implicit variable and the intensity integrated along Q_2 to improve the statistical quality of the data, and intensity as a function of $\{Q_1, \omega\}$ gives the full information of $S(\mathbf{Q}, \omega)$. These techniques have been used to study spin dynamics in single crystals since the early 1990s [30–33], and full mapping of excitations in quasi-2D materials became possible with the advent of the large position sensitive detector array of the MAPS spectrometer [34,35]. They are now routine on time-of-flight spectrometers around the world to study excitations in quasi-1D [11–16] and quasi-2D magnets [17–21] as well as copper based [2–5] and iron based [6–10] superconductors and their parents. Well-established software applications, such as DAVE [36], MSlice [37], and Utsusemi [38] exist to visualize and to perform some analysis of the data. Though it is possible to use the same techniques and software tools to analyze data from 3D materials [39,40], such analysis is far from routine.

In the case of MERLIN the number of detector elements is ≈70, 000, which is typical of the number for similar instruments at other sources, and the energy transfer axis is typically divided into